EES Solar

REVIEW

View Article Online
View Journal



Cite this: DOI: 10.1039/d6el00065g

# Supramolecular engineering-empowered safe, efficient, and stable perovskite solar cells

Jiarong Wang,[ac] Xian-Yin Dai,[d] Leyu Bi,[ab] Qiang Fu *[ace] and Alex K.-Y. Jen *[abc]

Perovskite solar cells (PSCs), an emerging photovoltaic technology, have achieved power conversion efficiencies (PCE) exceeding 27%, demonstrating significant application potential. However, their commercialization remains constrained by critical bottlenecks, including high defect-state density, uncontrollable crystallization processes, insufficient long-term stability, and lead-leakage risks. Supramolecular chemistry provides an innovative approach to addressing these challenges through non-covalent self-assembly strategies based on hydrogen bonding, π–π stacking, electrostatic interactions and van der Waals forces. This review systematically summarizes recent advances in supramolecular strategies for PSCs, focusing on defect passivation, crystallization regulation, stability enhancement, and lead-ion anchoring. It comprehensively analyzes the molecular design principles, working mechanisms, and advanced characterization techniques of representative materials. Rationally designed supramolecular systems effectively passivate surface and grain boundary defects, modulate crystallization kinetics, and enhance device stability under harsh conditions, including high temperature, high humidity, and light exposure. At the same time, they efficiently suppress lead ion migration and leakage through targeted trapping mechanisms. This review discusses the advantages and limitations of these strategies, offering theoretical insights and practical guidance for developing high-efficiency, stable, and environmentally friendly PSCs.

Received 4th April 2026
Accepted 5th May 2026

DOI: 10.1039/d6el00065g

rsc.li/EESSolar



## Broader context

The rapidly growing demand for clean, sustainable energy has driven intensive research into advanced photovoltaic technologies capable of efficiently harnessing abundant solar energy while mitigating pressing environmental concerns. Among these technologies, metal halide perovskite solar cells (PSCs) have emerged as one of the most promising next-generation photovoltaic systems, garnering widespread attention due to their certified power conversion efficiencies exceeding 27%, tunable band gaps, and low-cost, solution-processable fabrication. Nevertheless, the commercialization of PSCs remains severely constrained by persistent challenges, including high defect densities, poorly controlled crystallization processes, insufficient long-term operational stability, and potential environmental risks arising from lead leakage. Traditional covalent modification strategies often struggle to address these interrelated, complex issues comprehensively. In this context, supramolecular engineering, based on dynamic and reversible non-covalent interactions such as hydrogen bonding, π–π stacking, electrostatic interactions, and host–guest recognition, has increasingly been recognized as a powerful and versatile approach for achieving synergistic improvements in efficiency, stability, and environmental safety. This review systematically summarizes recent advances in supramolecular strategies aimed at overcoming key commercialization barriers in PSCs, with particular emphasis on the distinctive advantages of non-covalent molecular design over conventional covalent approaches, the fundamental mechanisms underlying defect passivation, crystallization regulation, stability enhancement, and lead ion immobilization, as well as the remaining scientific and technological challenges and future directions toward reliable, high-performance, and environmentally friendly perovskite photovoltaic devices.

## 1. Introduction

Since their first report in 2009, perovskite solar cells (PSCs) have experienced a significant increase in power conversion efficiency from 3.8% to over 27%, emphasizing their exceptional commercial potential.[1–6] This breakthrough stems from the unique crystal structure and outstanding optoelectronic properties of perovskite materials, including direct bandgaps, high extinction coefficients, long carrier diffusion lengths, and remarkable defect tolerance.[7–11] Although PSCs have higher efficiency than traditional silicon-based photovoltaics, they still face major challenges for large-scale deployment.[12–14] These

[a]Department of Materials Science and Engineering, City University of Hong Kong, Kowloon 999077, Hong Kong. E-mail: alexjen@cityu.edu.hk
[b]Department of Chemistry, City University of Hong Kong, Kowloon 999077, Hong Kong
[c]Hong Kong Institute for Clean Energy, City University of Hong Kong, Kowloon 999077, Hong Kong
[d]School of Chemistry and Pharmaceutical Engineering, Shandong First Medical University and Shandong Academy of Medical Sciences, Taian, 271016, China
[e]The Centre of Nanoscale Science Technology, Key Laboratory of Functional Polymer Materials (Ministry of Education), Frontiers Science Center for New Organic Matter (Ministry of Education), College of Chemistry, Nankai University, Tianjin 300071, China. E-mail: qfu@nankai.edu.cn

include non-radiative recombination losses caused by interfacial defects, poor control of crystallization dynamics, poor stability under heat, humidity, and light stress, and environmental toxicity issues due to lead in the light absorbers.[15–19] These issues critically impede the transition from lab-scale champion devices to industrial products and obstruct the pivotal shift from efficiency to reliability.[20–22]

Supramolecular chemistry offers a transformative approach to addressing these challenges through molecular assembly driven by non-covalent interactions, including hydrogen bonding, π–π stacking, and van der Waals interactions.[23–25] Its core advantage lies in the dynamic, reversible nature of weak interactions, enabling precise self-assembly and functional tunability to construct well-defined, multifunctional supramolecular architectures.[26,27] Such systems exhibit dynamic responsiveness, interfacial modifiability, and synergistic functionalities that allow simultaneous defect passivation, crystallization regulation, mechanical stress buffering, and lead-ion anchoring, all without compromising the intrinsic optoelectronic properties of perovskites.[28–30] For instance, functionalized macrocycles, such as cyclodextrins and crown ethers, can simultaneously passivate undercoordinated lead ion defects and immobilize lead ions through host–guest recognition or coordination interactions. This dual action significantly boosts device efficiency while improving environmental safety.[31–33]

In recent years, supramolecular strategies have made significant breakthroughs in PSCs.[34] A variety of supramolecular materials have been successfully deployed for defect passivation, modulation of crystallization kinetics, interfacial stabilization, and suppression of lead leakage.[35,36] These advances not only deepen our understanding of interfacial charge behavior and degradation mechanisms but also provide critical technical support for industrialization.[37,38] Compared to conventional material modification approaches, supramolecular chemistry, owing to its molecular programmability and functional integration, offers unique advantages for addressing complex, multiscale challenges.[39,40] As research progresses, this strategy is increasingly recognized as a key enabler of PSC commercialization.[41,42] This review comprehensively surveys the pivotal advances in supramolecular engineering for PSCs, focusing on mechanistic insights and performance outcomes in four core areas: defect passivation, crystallization control, stability enhancement, and lead leakage mitigation. Through detailed comparative assessments of diverse supramolecular systems and forward-looking discussions on current limitations, we aim to provide a robust theoretical foundation and a practical roadmap for developing efficient, stable, and environmentally friendly perovskite photovoltaics.

## 2. Concepts and characteristics of supramolecular chemistry

Supramolecular chemistry is a discipline dedicated to the study of molecular assemblies governed by non-covalent interactions, encompassing their properties, structures, synthesis, applications, and interconversions.[43] Key supramolecular interactions include hydrogen bonding, π–π stacking, electrostatic forces, and van der Waals interactions (Fig. 1).[44] Although individually weak (typically 0.1–50 kcal $mol^{-1}$), these interactions exhibit reversibility, directionality, and selectivity.[45] Through cooperative effects, they enable precise structural and functional control at the molecular level, facilitating the construction of tailored supramolecular systems with specific functionalities.[46] This differs from traditional covalent polymers or permanently cross-linked networks, unless their function in PSCs is primarily dominated by supramolecular assembly rather than irreversible chemical bonding.

This section systematically categorizes these interactions, highlights representative functional materials, and discusses the characterization strategies employed.

### 2.1 Key interaction mechanisms

Different supramolecular interactions exhibit varying binding strengths, orientations, selectivities, and dynamic behaviors, thereby playing distinct mechanistic roles in PSCs. Understanding the synergistic effects of different interaction types is crucial for the rational design of supramolecular systems in perovskite solar cells.

**2.1.1 Hydrogen bonding.** Hydrogen bonding, one of the most critical supramolecular interactions, exhibits moderate binding strength, strong directionality, high selectivity, and dynamic adjustability.[47–49] By introducing functional groups such as hydroxyl (–OH), amino (–$NH_2$), or carboxyl (–COOH), stable hydrogen-bond interactions can form with cations (*e.g.*, $MA^+$ and $FA^+$) on the perovskite surface, thereby optimizing interfacial energy-level matching.[50,51] Simultaneously, hydrogen bonds can passivate defect sites in the perovskite film, reducing non-radiative recombination losses and improving carrier lifetime and device efficiency.[52] Furthermore, by introducing appropriate materials into the precursor, the perovskite nucleation and crystallization process can be regulated through hydrogen bonding to obtain high-quality films. For example, Li *et al.* added a multifunctional molecule (4-guanidinobenzoate)

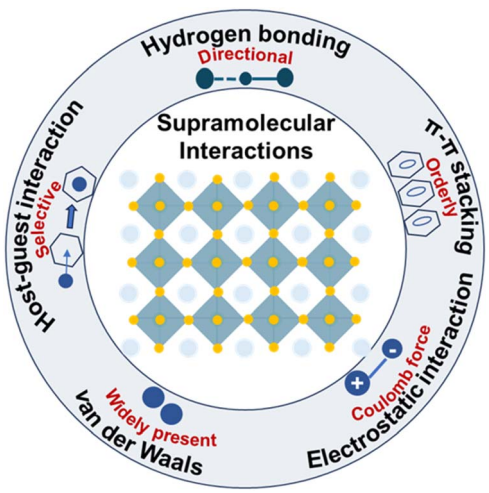


Fig. 1 Key supramolecular interactions.

to the perovskite precursor, which regulated the crystal growth kinetics of perovskite by forming hydrogen bond bridging intermediates, promoted the formation of large-sized perovskite grains, and suppressed non-radiative recombination of the film.[25] Similarly, Qin *et al.* designed a multifunctional fluorinated additive that can be polymerized *in situ*, which can not only inhibit complex intermediate phases and promote the directional crystallization of the perovskite α phase, but also polymerize *in situ* during the formation of perovskite films to form a hydrogen bond network to stabilize the α phase (Fig. 2a).[53] Additionally, organic ligands introduced *via* hydrogen bonding can form a protective layer on the perovskite surface, thereby suppressing ion migration and phase transitions, which improves the long-term stability of the device. Liu *et al.* used a series of organic spacer cations to induce a mixed linkage structure by introducing interspacer interactions (*e.g.*, π–π interactions and hydrogen bonds), thereby forming a two-dimensional perovskite-type protective layer on the three-dimensional perovskite surface.[54] This effectively passivated the perovskite surface, allowing for the preparation of uniform, large-area perovskite films.

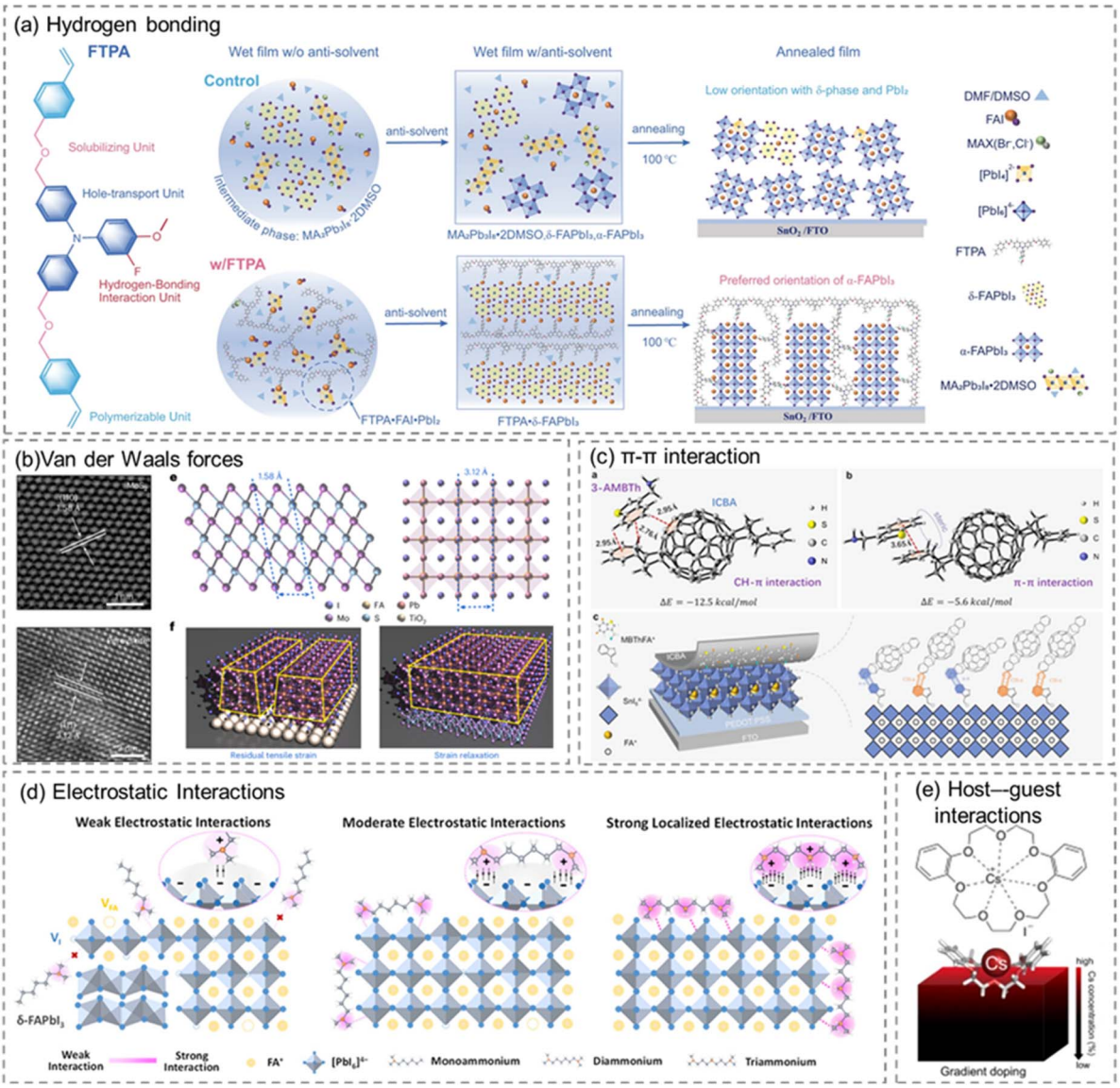


Fig. 2 Applications of supramolecular interactions in PSCs. (a) Hydrogen bonding: the regulated crystallization process of FA-based perovskite *via* hydrogen-bonded polymer networks. Adapted from ref. 53 with permission from Springer Nature,[53] Copyright 2023. (b) Van der Waals forces: schematic diagram of perovskite film growth on $MoS_2$. Adapted from ref. 61 with permission from Springer Nature,[61] Copyright 2024. (c) π–π interaction: schematic diagram of charge-bridging pathways constructed at the perovskite/ICBA interface through interface modification by 3-AMBTh. Adapted from ref. 62 with permission from Wiley,[62] Copyright 2024. (d) Electrostatic interactions: a schematic illustration of a strong localized electrostatic interaction stabilizing the perovskite structure. Adapted from ref. 63 with permission from Wiley,[63] Copyright 2025. (e) Host–guest interactions: schematic representation of the gradient and homogeneous Cs doping of perovskite films. Adapted from ref. 64 with permission from Springer Nature,[64] Copyright 2021.

**2.1.2 Van der Waals forces.** The van der Waals force is a ubiquitous weak intermolecular interaction that plays an important auxiliary role in supramolecular assembly and the interfacial stability of PSCs.[55] They facilitate non-specific adsorption on perovskite surfaces and enhance the packing stability of supramolecular aggregates, collectively contributing to stable supramolecular interface formation.[56,57] Van der Waals forces can influence the growth direction and morphology of perovskite crystals.[58] By introducing organic ligands or 2D materials with strong van der Waals effects (such as graphene and transition metal dichalcogenides), the crystallization process of perovskite films can be regulated, resulting in denser and more ordered structures.[59] Furthermore, van der Waals forces can promote close contact at the perovskite/charge transport layer interface, thereby facilitating charge transfer and improving device efficiency.[60]

For example, Koo *et al.* proposed mesoporous $MoS_2$ as a highly efficient and stable ETL material (Fig. 2b).[61] The mesoporous $MoS_2$ intermediate layer provides a larger surface contact area with the perovskite capping layer, thereby improving charge extraction efficiency at the perovskite layer–ETL interface.[61] In addition, the $MoS_2$ layer can serve as an ideal template, promoting the van der Waals epitaxial growth of perovskites with well-matched lattice parameters, thus significantly improving the crystallinity of the capping perovskite and significantly reducing residual strain.[65]

**2.1.3 π–π stacking.** π–π stacking is fundamentally a subtype of van der Waals forces, formed between aromatic rings or conjugated systems through the overlap of molecular orbitals.[66–68] Its strength is influenced by the degree of π-conjugation, spatial orientation, and stacking geometry.[69,70] Notably, π–π stacking exhibits significant directionality and relatively high binding energy, highlighting its importance in molecular assembly and materials design.[71,72] In PSCs, π–π stacking can enhance molecular interactions and improve carrier mobility, thereby optimizing the charge-transport layer.[73,74] By introducing materials with strong π–π stacking ability (such as fullerene derivatives), an ordered molecular arrangement can be formed on the perovskite surface, optimizing the interface charge transport characteristics.[75–77] In 2D/3D perovskite heterostructures, aromatic spacers utilize π–π stacking to induce ordered layered architectures that simultaneously passivate defects and provide hydrophobic shielding.[78–81] At interfaces, aromatic molecules self-assemble into monolayers that improve charge transport.[82] In hole-transport materials, π-conjugated polymers form continuous charge pathways through ordered stacking, markedly enhancing carrier mobility.[83,84]

For example, Jen *et al.* designed new carbazole-derived self-assembling monolayers (SAMs), CbzPh and CbzNaph, *via* asymmetric or helical π-expansion, whose stronger π–π interactions yield more ordered, denser SAM assemblies.[85] Hu *et al.* introduced 3-aminomethylbenzo[*b*]thiophene (3-AMBTh) into perovskite films *via* a simple post-growth process to construct charge transfer pathways (Fig. 2c).[62] The selective reaction of 3-AMBTh with exposed $FA^+$ on the perovskite surface suppressed the formation of iodine vacancy defects, thereby reducing the trap density. Furthermore, the residual aromatic rings on the surface formed an effective π–π stacking interaction system with subsequently deposited ICBA, promoting charge transfer at the interface.

**2.1.4 Electrostatic interactions.** Electrostatic interactions are Coulomb forces between charged molecules or ions. Depending on the polarity of the charge, strong attraction or repulsion occurs. By introducing functional materials with positive or negative charges (*e.g.*, polycationic or anionic polycationic materials), the energy-level matching between the perovskite layer and the charge-transport layer can be tuned, thereby optimizing carrier-separation efficiency and regulating interfacial energy levels.[86] Cationic surfactants adsorb onto negatively charged perovskite surfaces *via* electrostatic attraction, forming an electrical double layer that can not only passivate defects but also modulate the surface work function.[87,88] Furthermore, crown ether plasma carriers utilize electron-rich cavities to form "electrostatic coordination" complexes, selectively binding cations to effectively suppress ion migration and improve device stability.[89]

For example, Ge *et al.* employed zwitterion elastomers, 3-[[2-(methacryloyloxy)ethyl]dimethylammonio]propane-1-sulfonate (SBMA), as novel adhesives and self-healing additives in perovskite films.[90] The highly electronegative sulfo-end groups on SBMA induced a substantial dipole moment in the molecule, facilitating dielectric screening during the carrier capture process, thus effectively suppressing non-radiative recombination in PSCs. Li *et al.* enhanced local electrostatic interactions that stabilize the perovskite structure by introducing a novel, carefully designed tetramethyldisyltriammonium cation (Fig. 2d).[63] This cation not only exhibits stronger electrostatic interactions with the $[PbI_6]^{4-}$ octahedron but also possesses multi-site interactions with significant steric hindrance, enabling it to bind with the perovskite. Therefore, this strong local electrostatic interaction induces lattice compression and increases the perovskite lattice energy by enhancing the chemical bonding between $FA^+$ and $[PbI_6]^{4-}$ and shortening the Pb–I bond. This synergistic suppression of ion migration under various external stresses ultimately improves structural stability.

**2.1.5 Host–guest interactions.** Host–guest interaction refers to the interaction between a host molecule and a guest molecule, mediated by a variety of weak interactions (such as van der Waals forces, hydrogen bonds, and electrostatic interactions).[91] It exhibits high selectivity and inclusiveness and is often employed in molecular recognition and assembly.[92] In PSCs, the use of host molecules, such as crown ethers, to wrap cations or defect sites on the perovskite surface can form a stable interface structure, thereby reducing non-radiative recombination (Fig. 2e).[64] Additionally, the introduction of functional ligands through host–guest interactions can effectively passivate the trap states in the perovskite film, thereby improving the carrier lifetime and device efficiency.[93] In practical applications, multiple supramolecular interactions usually work synergistically. For example, hydrogen bonds and van der Waals forces work together to stabilize the interface structure.

π–π stacking and electrostatic interactions optimize charge transfer properties.[94] Host–guest interactions and other weak interactions work together to passivate defects.

### 2.2 Representative supramolecular materials

**2.2.1 Cyclodextrins (CDs).** Cyclodextrins (CDs) are naturally occurring cyclic oligosaccharides composed of D-glucose units linked by α-glycosidic bonds. They possess a cyclic structure with a hydrophobic internal cavity and a hydrophilic external surface.[95,96] Common cyclodextrins include α-, β-, and γ-cyclodextrins, which vary in cavity size due to differences in the number of glucose units, allowing them to selectively encapsulate various molecules (Fig. 3a).[97] Chemical modifications of cyclodextrins can modulate their solubility, binding affinity, and functional diversity.[98–100] For example, CD molecules can be modified with functional groups to enhance the hydrophilicity of CDs, making them useful in aqueous environments, or introduce hydrophobic moieties to improve the binding affinity for specific guest molecules.[101,102] In PSCs, CDs can form supramolecular complexes with components in perovskite materials through host–guest complexation or regulate the crystallization process of perovskite through hydrogen bond interactions.

**2.2.2 Crown ethers (CEs).** Crown ethers (CEs) are cyclic oligomers of ethylene oxide containing multiple electron-donating heteroatoms that can selectively coordinate with metal cations within their central cavities (Fig. 3b).[103–105] The cavity size determines ion selectivity, allowing preferential binding of specific cations. For example, 18crown-6 has a high affinity for $K^+$, 15crown-5 has a high affinity for $Na^+$, and 12crown-4 has a high affinity for $Li^+$ ions. Notably, CEs containing only neutral oxygen donor atoms are well-suited for binding to alkali, alkaline earth, and some post-transition metal ions.[106] Structural modifications, including heteroatom substitution, can further enhance the dipole moment and coordination strength.[31,107] CE can form a coordination bond with the metal ions in the perovskite material *via* the internal cavity, thereby modulating crystallization, passivating defects, and stabilizing the perovskite structure, thereby improving device performance and operational stability.[108] Substituting heteroatoms can yield a larger dipole moment, thereby enhancing coordination interactions with lead cations.

**2.2.3 Calixarenes.** Calixarenes are a class of wheel-shaped supramolecular structures composed of several phenol units linked by methylene bridges (and variants such as sulfide bridges) (Fig. 3c). Their hydrophobic cavities effectively trap cations, including potassium ($K^+$), sodium ($Na^+$), methylammonium ($MA^+$), and formamidinium ($FA^+$). This chelation inhibits cation migration and prevents their decomposition under high-temperature, high-humidity conditions. Liu *et al.* proposed a supramolecular confinement method.[109] Assembling calixarene end-capping layers on the precursor surface can induce host–guest interactions with solvent molecules, thereby regulating desolvation kinetics and initiating perovskite crystallization from a straightforward molecular–precursor interface. These combined effects significantly reduce the spatial variability of perovskite films and broaden their processing window. This enables the reproducible fabrication of highly crystalline, ultra-smooth perovskite films.

**2.2.4 Cucurbit[*n*]urils (CB[*n*]).** Cucurbiturils are a class of highly symmetrical, rigid, pumpkin-shaped macrocyclic host molecules composed of multiple glycoluril units bridged by methylene groups in the form of CB[*n*], where *n* represents the number of glycoluril units (Fig. 3d). The structure features a polar, hydrophobic inner cavity and negatively charged carbonyl groups at the edges of two portals, which can provide access to the hydrophobic cavity.[110] They readily accommodate cations or neutral guests. In PSCs, CB[*n*] stabilizes lattice cations *via* host–guest interactions, reducing non-radiative recombination and enhancing charge transport, thereby improving both efficiency and stability.[111]

Supramolecular material design centers on the engineering of functional groups, the optimization of molecular architecture, and the control of self-assembly behavior. Functional groups dictate chemical reactivity, molecular structure governs conformational flexibility, and self-assembly is modulated by concentration, solvent, and temperature. In PSCs, these materials are primarily used in interfacial engineering, bulk doping, and encapsulation to passivate defects, align energy levels, and enhance long-term stability without degrading intrinsic optoelectronic performance.

### 2.3 Characterization techniques for supramolecular interactions

Quantitative and visual characterization of supramolecular interactions relies on the integration of spectroscopy, thermodynamics, structural chemistry, and theoretical chemistry to elucidate the driving mechanisms of non-covalent interactions (hydrogen bonds, van der Waals forces, π–π stacking, electrostatic interactions, and host–guest interactions) in molecular recognition and self-assembly at different spatiotemporal scales.

Nuclear magnetic resonance (NMR) reveals binding sites and conformational changes through chemical shifts and exchange kinetics.[112] It is widely used for identifying host–guest complex systems and hydrogen bonds.[113] Fourier transform infrared spectroscopy (FT-IR) and Raman spectroscopy can capture characteristic peak shifts and band shapes of vibrational levels induced by hydrogen bonding and coordination, making them particularly suitable for resolving weak interactions between hydroxyl, carbonyl, and metal-coordinating groups. Ultraviolet visible spectroscopy and steady-state/time-resolved fluorescence spectroscopy can provide intuitive insights into electronic structure perturbations and energy transfer. When guest molecules enter hydrophobic cavities and undergo π–π stacking or charge transfer, the peak positions, intensities, and lifetimes of absorption and emission spectra exhibit regular shifts and quenching/enhancement. This spectral response typically complements the site information provided by nuclear magnetic resonance (NMR), thus offering dual evidence for "electronic conformation." Thermal and structural analyses include differential scanning calorimetry (DSC) and

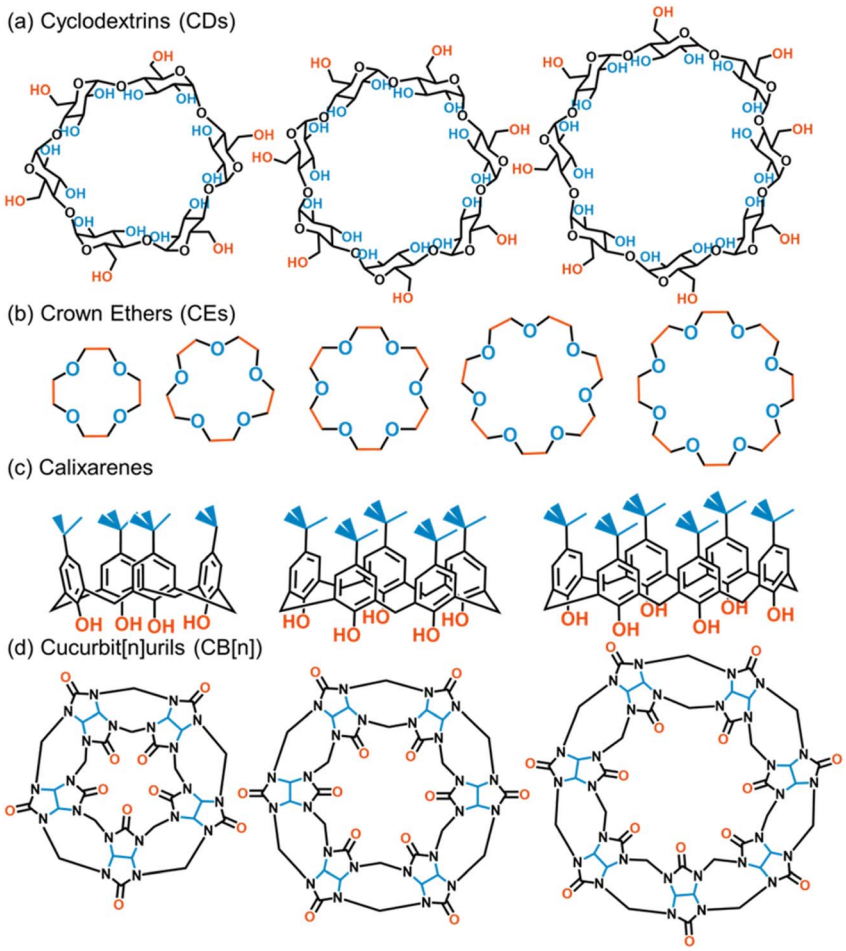


Fig. 3 The chemical structures of representative supramolecular materials. (a) Cyclodextrins. (b) Crown Ethers. (c) Calixarenes. (d) Cucurbit[*n*] urils. Red sites are easier to modify, while blue sites are more challenging.

thermogravimetric analysis (TGA) to assess thermal stability, as well as X-ray diffraction (XRD) and scanning electron microscopy/transmission electron microscopy (SEM/TEM) to characterize the crystal structure and morphology. Dynamic light scattering (DLS) and cyclic voltammetry (CV) are used to assess aggregation and charge transfer dynamics. These experimental data are supplemented by molecular dynamics (MD) simulations and density functional theory (DFT) calculations to simulate interaction mechanisms at the quantum level.

## 3. Applications of supramolecular materials in PSCs

### 3.1 Defect passivation

Defect passivation is a cornerstone strategy for enhancing PCE and long-term stability in PSCs. Researchers have developed efficient supramolecular systems based on hydrogen bonding, coordination, host–guest inclusion, and co-assembly. He *et al.* developed a multifunctional universal ion migration suppression strategy (Fig. 4a) that, through host–guest interactions mediated by calixarene supramolecular structures, simultaneously suppresses the migration of $FA^+$, $I^-$, $Li^+$, and $Ag^+$ *via* coordination and hydrogen bonds, thereby stabilizing the perovskite layer, hole transport layer (HTL), and metal electrode layer.[114] Furthermore, C8A can promote p-type doping of Spiro-OMeTAD and passivate interface defects, thereby promoting hole extraction and transport and suppressing trap-assisted non-radiative recombination.

Crown ethers have also been widely used due to their cavity structure and affinity for cations. Su *et al.* used crown ethers to modulate perovskite films, thereby passivating surface defects that were insufficiently coordinated (Fig. 4b).[93] Crown ethers induce host–guest complex formation at the surface of perovskite films, reducing trap-state density at the hole-transport layer and grain boundaries and thereby significantly suppressing the performance loss in solar cells caused by non-radiative recombination. PSCs regulated by crown ethers exhibit higher operational stability and power conversion efficiencies exceeding 23%. Zhao *et al.* employed dibenzo-21-crown-7 in a dual host–guest strategy that concurrently passivated lattice defects and formed a protective surface layer, yielding certified PCEs of 25.5% with exceptional stability.[64] Nitrogen-doped crown ethers further optimized $Pb^{2+}$ coordination *via* enhanced dipole moments. Yang *et al.* found that nitrogen-

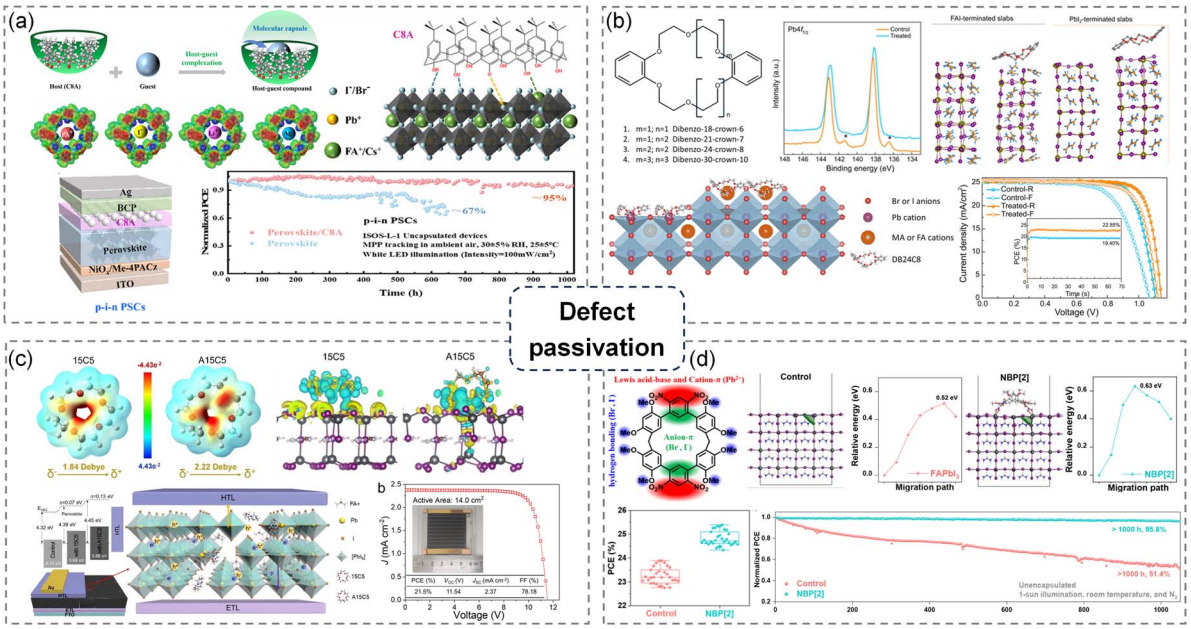


Fig. 4 (a) Ion migration inhibition strategies based on host–guest interactions between C8A and various mobile chemical substances. Adapted from ref. 114 with permission from Wiley,[114] Copyright 2025. (b) Regulation mechanisms and action sites of benzannulated crown ethers on perovskite films. Adapted from ref. 93 with permission from American Chemical Society,[93] Copyright 2020. (c) Regulation strategies of aza-crown ethers on perovskite films. Adapted from ref. 115 with permission from Wiley,[115] Copyright 2024. (d) Tailored Electron-Deficient Macrocycles Guiding the Perovskite Crystallization Process for Solar Cells. Adapted from ref. 116 with permission from American Chemical Society,[116] Copyright 2025.

doped A15C5 has a larger dipole moment than 15C5, and due to its electron-donating ability to soft Lewis acids, it has a stronger coordination ability with lead cations (Fig. 4c).[115] This improves the uniformity, defect passivation ability, and electronic performance of the film. Ultimately, PSCs containing A15C5 achieved a power conversion efficiency (PCE) of 25.0%, demonstrating good operational and environmental stability. A PCE of 21.5% was achieved on an active area of 14.0 $cm^2$.

Furthermore, more types of supramolecular functional materials have been used to regulate the quality of perovskite films. β-Cyclodextrin passivates undercoordinated $Pb^{2+}$ through hydroxyl coordination and encapsulates residual $PbI_2$, promoting uniform crystallization and moisture resistance. Macrocycles, such as cryptand C222, construct "lead cages" to immobilize $Pb^{2+}$, thereby suppressing deep traps and ion migration. Qiu *et al.* developed a novel electron-deficient biphenyl[*n*]aromatic macrocyclic molecule (NBP). When introduced into perovskite, it can regulate the perovskite crystallization process and inhibit halide-ion migration (Fig. 4d).[116] In addition, NBP can also effectively bind to uncoordinated halide ions and $Pb^{2+}$, reducing inherent defects through Lewis acid–base interactions and cation-π interactions. Self-assembled monolayers (SAMs) with Lewis-basic groups enable simultaneous interfacial energy-level tuning and defect passivation. Collectively, these supramolecular approaches enable precise, multi-level defect management, laying a solid foundation for commercial deployment under harsh environmental conditions.

### 3.2 Crystallization control

The quality of perovskite films is exquisitely sensitive to nucleation rate, crystal orientation, and phase purity. Supramolecular reagents can precisely control the crystallization process through host–guest complexation, hydrogen bonding, and electrostatic interactions.[117,118] β-cyclodextrin (CD) derivatives selectively recognize precursors through inclusion interactions, achieving comprehensive control over crystallization, passivation, and stability.

Zeng *et al.* prepared a supramolecular interface layer by introducing the three-dimensional multidentate ligand methyl-β-cyclodextrin (methyl-β-CD) onto poly(3,4-ethylenedioxythiophene):poly(styrene sulfonate) (PEDOT:PSS).[40] This supramolecular interface layer achieved good crystallization control (fast nucleation, slow growth) (Fig. 5a). Specifically, the weak coordination between CD and ammonium at the supramolecular interface promoted the nucleation rate, while multisite interactions in different spatial directions inhibited crystal growth, resulting in a denser tin perovskite film with fewer defects. Wang *et al.* introduced thiol-modified β-CD (β-CD-$(SH)_7$) into the perovskite precursor solution.[119] The thiol modification enhanced its interaction with perovskite precursors, effectively regulating the nucleation and crystallization process of the perovskite, resulting in films with excellent quality and lower defect density.

Crown ethers coordinate with metal cations through the lone pair electrons of oxygen atoms within their ring cavities, forming stable coordinate bonds and generating positively charged sites on the molecular framework. These sites strongly attract

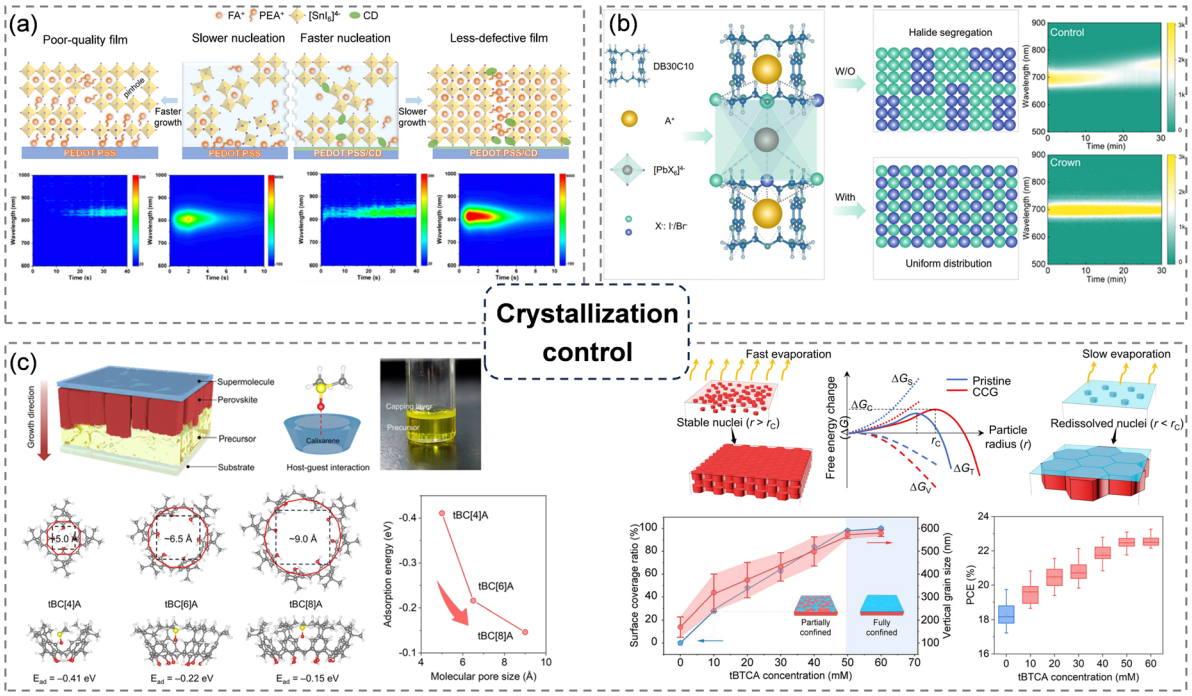


Fig. 5 (a) Nucleation and crystallization processes of tin perovskite on PEDOT:PSS and PEDOT:PSS/CD substrates. Adapted from ref. 40 with permission from American Chemical Society,[40] Copyright 2025. (b) Schematic diagram of halogen modulation in perovskite without and with Crown. Adapted from ref. 41 with permission from Springer Nature,[41] Copyright 2025. (c) A schematic diagram of perovskite thin film formation under a capping layer (supramolecular confinement growth). Adapted from ref. 109 with permission from Springer Nature,[109] Copyright 2025.

and stabilize halide ions, thereby suppressing halide ion migration in wide-bandgap (WBG) perovskites. For example, Lian *et al.* used macrocyclic dibenzo-30-crown ether-10 (DB30C10) molecules as additives to effectively regulate crystallization kinetics and suppress halide segregation under illumination (Fig. 5b) by adjusting the coordination of halides with monovalent cations and lead ions.[41] Ultimately, the supramolecularly engineered 1.77 eV PSCs achieved a champion power conversion efficiency (PCE) of 21.01% and exhibited excellent operational stability, maintaining 95% of their initial efficiency after 1000 hours of maximum power point tracking. Chen *et al.* introduced crown ethers into perovskite precursors.[117] Due to the strong interactions between crown ethers and $Cs^+$ and $Pb^{2+}$ metal ions, the crystallization process was effectively regulated, promoting uniform nucleation and growth of pure-phase perovskite films.

Furthermore, the supramolecular confinement effect mediated by thiocalixarenes guided epitaxial growth and slowed ion diffusion, thereby improving the orientation and uniformity of the films.[109] Liu *et al.* constructed a straightforward calixarene–precursor interface to regulate the formation kinetics of perovskite. This interface, rather than an air–precursor interface or a bulk precursor film, was able to initiate perovskite growth (Fig. 5c). This unique molecularly permeable capping layer regulates desolvation kinetics through host–guest interactions and confines perovskite formation below a flat interface, thereby achieving the reproducible preparation of highly crystalline, ultra-smooth perovskite films. Zhang *et al.* used 4-*tert*-butyl-1-(ethoxycarbonyl-methoxy)thiocalix4arene (*t*BuTCA) to form host–guest complexes with cations and extracage lead iodide(II) ($PbI_2$).[118] At the same time, the negative charge compensation of iodine vacancies can suppress the formation of Pb–Pb dimers, thereby significantly inhibiting non-radiative complexation. Polymer templates, such as ethyl cellulose, promote large-grain formation through hydrogen bonding. Real-time monitoring *via in situ* XRD and PL has revealed the microscopic mechanisms from nucleation kinetics to phase-purity control, providing vital guidance for high-quality film fabrication.

### 3.3 Stability enhancement

PSCs have revolutionized the photovoltaic landscape owing to their remarkable power conversion efficiencies (PCEs). However, operational stability remains a critical barrier to commercialization.[38] A primary degradation pathway involves light- and heat-induced decomposition of the perovskite phase into metallic $Pb^0$ and volatile iodine species ($I_2/I^0$). The escape of $I_2$ not only compromises lattice integrity but also corrodes charge transport layers (CTLs) and electrodes.[33] Moreover, volatilized $I_2$ can react with $I^-$ to form polyiodides ($I_x^-$), which generate radicals under illumination, triggering a self-accelerating cascade of decomposition reactions. Concurrently, the aggregation of $Pb^0$ promotes non-radiative recombination.[31,34]

β-Cyclodextrin is often used as an iodine scavenger; its suitable pore size and unique hydrophobic cavity structure

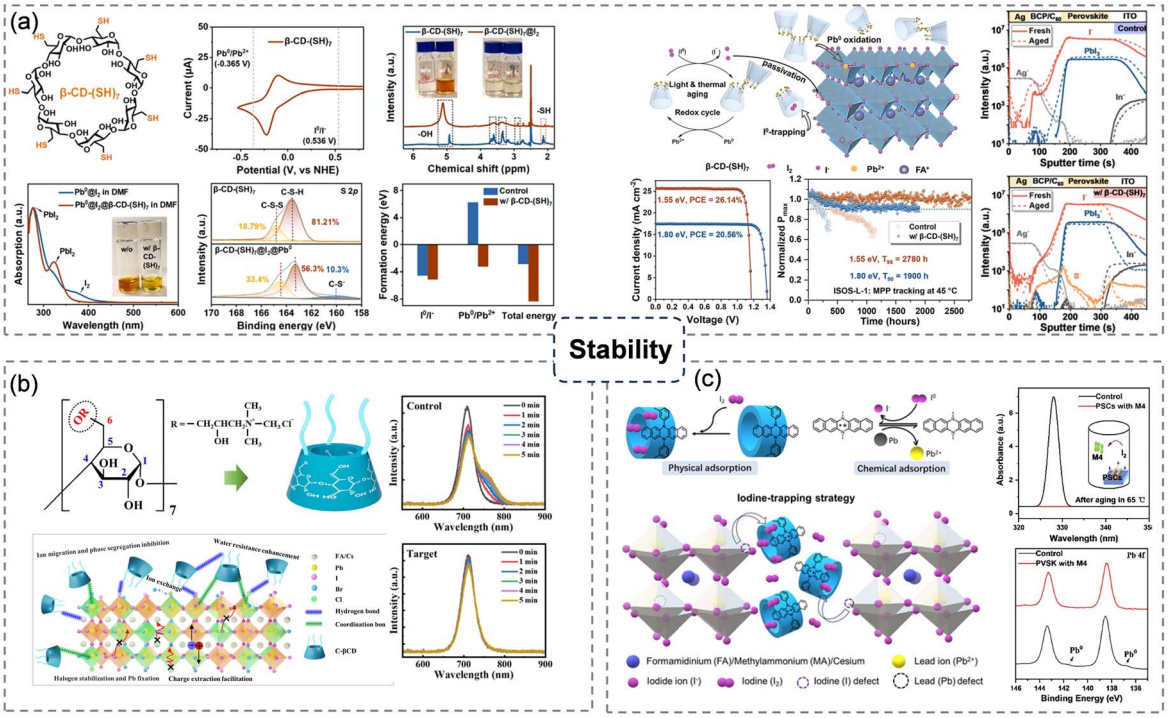


Fig. 6 (a) Thiol-functionalized β-CD as redox shuttles enhances the photothermal stability of PSCs. Adapted from ref. 119 with permission from Elsevier.[119] Copyright 2025. (b) Functionalized cationic β-CD stabilizes halide ions in wide-bandgap perovskites, homogenizes the phase distribution, and effectively immobilizes $Pb^{2+}$ ions. Adapted from ref. 120 with permission from Wiley,[120] Copyright 2025. (c) Supramolecular macrocyclic iodine adsorbents enable photothermally stable PSCs. Adapted from ref. 37 with permission from Wiley,[37] Copyright 2025.

effectively capture iodine. Li *et al.* introduced it into perovskite films, effectively binding photogenerated iodine within the perovskite film and trapping it in its bowl-shaped structure, suppressing iodine escape at high temperature.[33] Notably, it was verified that these captured iodines can also react with metallic $Pb^0$ to regenerate the perovskite phase, thereby inhibiting perovskite degradation. The resulting device maintained over 80% of its initial efficiency after 300 hours of MPP tracking at 85 °C. Wang *et al.* further modified β-CD with thiols, yielding β-CD-$(SH)_7$, which combines three synergistic effects: iodine confinement *via* supramolecular interactions, chemical redox cycling, and dynamic defect repair.[119] The β-CD cavity acts as a molecular trap, selectively capturing iodine through host–guest interactions, while its thiols (–SH) groups participate in redox cycles, reversibly reducing iodine to iodide ions and oxidizing lead to lead oxides through S–S bond formation. This dual mechanism prevents iodine loss and regenerates lead, thereby restoring the perovskite lattice and achieving dynamic defect repair (Fig. 6a). This strategy significantly improves the photothermal stability of the device. Yang *et al.* introduced a small amount of cationic β-cyclodextrin, composed of multiple ammonium cations, chloride ions, and abundant hydroxyl functional groups, into wide-bandgap perovskites (Fig. 6b). This synergistically stabilized halide ions and enhanced the immobilization effect of lead in high-bromine-content mixed halide wide-bandgap perovskites, outperforming traditional electrically neutral cyclodextrin chelating agents.[120] Therefore, halide segregation and phase separation were effectively suppressed, resulting in the preparation of high-quality, wide-bandgap perovskite films with enhanced chemical homogeneity and improved photoelectric properties. In addition to cyclodextrin molecules, Wu *et al.* also developed novel nitrogen-doped conjugated macrocyclic iodine adsorbents (M3 and M4).[37] Due to the electron-rich properties of the dihydrodia-pentabenzene unit and the well-defined cylindrical cavity of the macrocyclic compound, M3 and M4 exhibit a dual-mode iodine capture: chemisorption through charge–transfer interactions and physical encapsulation within the macrocyclic cavity. Furthermore, these macrocyclic compounds exhibit excellent iodine adsorption–desorption cycling performance, enabling the release of captured iodine and promoting the regeneration of perovskite (Fig. 6c). Zhang *et al.* constructed an "iodide buffer layer" in PSCs using a starch-polyiodide (Starch-I) supramolecular structure. This buffer layer retains sufficient iodide in the perovskite, thereby suppressing ion drift and repairing newly formed iodine vacancies, thus regulating the kinetics of halide migration during light–dark cycling. The fabricated device maintained 98% of its initial efficiency after 42 24-hour cycles (12 hours of light/dark) and 99% of its initial PCE after more than 1500 accelerated light–dark cycles (each lasting 20 minutes).[34] These advances demonstrate that supramolecular materials can not only enhance environmental adaptability through interface and bulk engineering but also serve as an essential bridge between basic research and industrial applications.

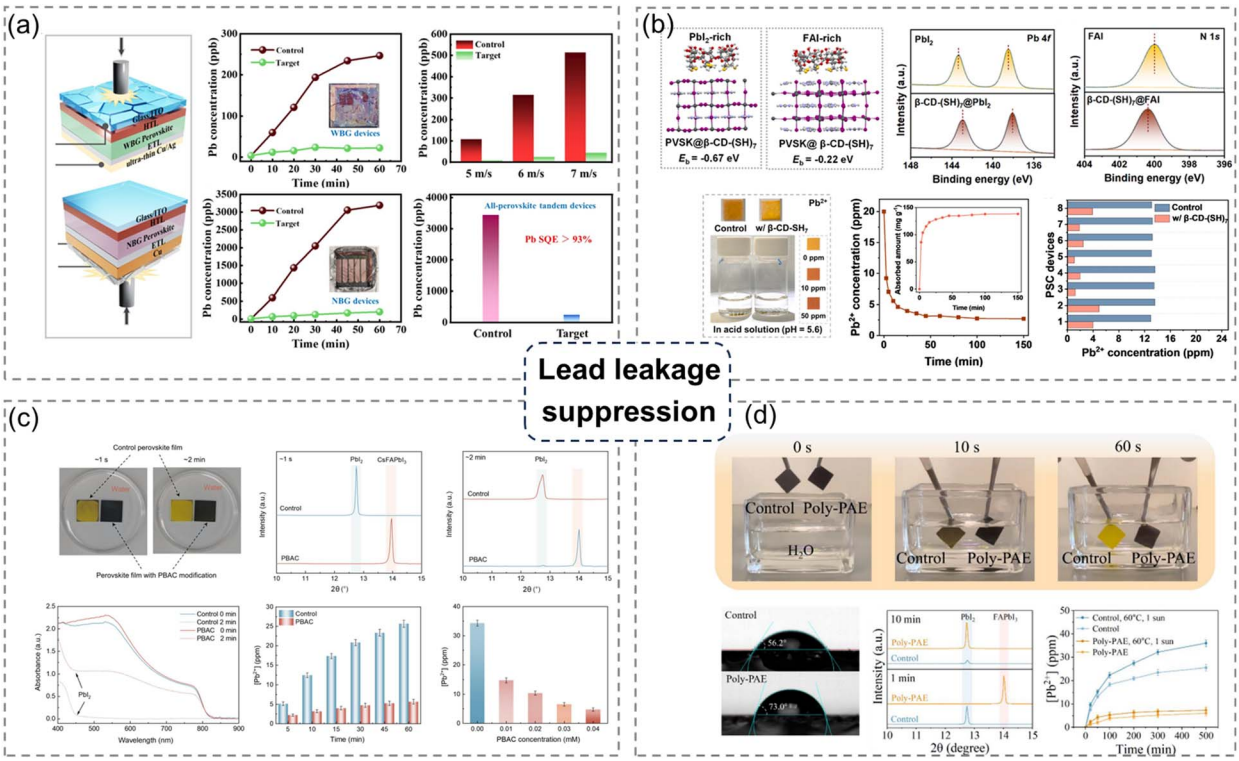


Fig. 7 (a) Functionalized cationic β-CD acts as a strong $Pb^{2+}$ binding agent, inhibiting lead leakage. Adapted from ref. 120 with permission from Wiley,[120] Copyright 2025. (b) Thiol-modified β-CD enhances its binding ability with Pb and inhibits lead leakage. Adapted from ref. 119 with permission from Elsevier,[119] Copyright 2025. (c) PBAC polymers suppress lead leakage through grain boundary encapsulation and strong bonding with lead. Adapted from ref. 121 with permission from American Association for the Advancement of Science,[121] Copyright 2025. (d) Poly-PAE inhibits lead leakage through the shielding effect of its double-chain copolymer network. Adapted from ref. 122 with permission from Wiley,[122] Copyright 2025.

### 3.4 Lead-leakage suppression

Lead leakage is a significant environmental hazard for the commercialization of perovskite photovoltaics, particularly when devices are damaged or exposed to humid and hot environments for extended periods, as $Pb^{2+}$ easily dissolves and contaminates water bodies.[123–125] Traditional physical encapsulations (such as glass and polymers) can delay water intrusion.[126,127] However, they cannot effectively capture leads and suppress leakage. Recent research suggests that supramolecular materials and their synergistic effects provide a novel approach to addressing this issue, both by suppressing instability during device operation and by rapidly encapsulating Pb after damage.[128,129] From an application perspective, related strategies can be categorized into two types: bulk-embedded supramolecular networks and external supramolecular encapsulation.[130,131] Functionalized cyclodextrin molecules show great potential in this regard. For example, cationic β-CD,[120] composed of multiple ammonium cations, chloride ions, and abundant hydroxyl functional groups, has been introduced into wide-bandgap perovskites, simultaneously stabilizing halide ions and immobilizing lead ions (Fig. 7a). Internal chemical encapsulation with cationic β-CD effectively prevents severe device damage and suppresses lead leakage during water immersion (lead leaching from single-junction devices is only 5.63 ppb, far below the US drinking water safety standard (<15 ppb)). Thiol-modified β-CD enhances its binding energy to lead. While stabilizing the perovskite lattice through dynamic bonds formed by thiols and disulfides, the device also adsorbs lead ions *in situ*, significantly suppressing lead leakage during water immersion (Fig. 7b). Quantitative analysis shows that β-CD-$(SH)_7$ exhibits excellent Pb adsorption performance, with an adsorption capacity ($q_e$) of 139.66 mg $g^{-1}$.[119] Yang *et al.* achieved deeper stabilization through internal encapsulation and chemical synergy.[36] Specifically, an internally integrated self-crosslinking supramolecular complex composed of 2-hydroxypropyl-β-cyclodextrin (HPβCD) and 1,2,3,4-butanetetracarboxylic acid (BTCA) was introduced into the bulk of the perovskite. The strong chemical coordination and multidentate chelation between the HPβCD-BTCA complex and $Pb^{2+}$ minimized lead leakage. They reduced lead toxicity in the resulting PSC. Building on this, replacing traditional glass-encapsulated devices with HPβCD-BTCA composites further reduces lead leakage from perovskite decomposition caused by rainwater and enhances the device's mechanical shock resistance under severe impact. Even after severe device damage, it retains 97% of its initial efficiency after 522 hours of dynamic water washing. Other functional materials, such as ionomer gels and cation-exchange resins, also inhibited lead leakage by chelating lead ions.[132]

Additionally, lead leakage can be reduced by stabilizing the perovskite phase. Zang *et al.* added the small organic compound *N*,*N*′-bis(acryloyl)cysteine (BAC) to the perovskite precursor solution, forming a polymer BAC (PBAC) at the perovskite grain boundaries during the annealing process of the perovskite film (Fig. 7c).[121] PBAC not only overcomes the limitations of small organic molecules but also enables it to interact with the perovskite through its abundant functional groups and multiple reaction sites. This interaction effectively passivates deep-level defects and suppresses non-radiative carrier recombination. The hydrophobic PBAC can encapsulate grain boundaries, effectively hindering direct contact and interaction between water and the perovskite, thereby preventing the collapse of the perovskite structure and slowing down the escape of $Pb^{2+}$. Similarly, Ma *et al.* designed a multifunctional additive with photosensitive properties, polyamide ester (PAE), which can form a unique double-chain copolymer network *via* UV-induced *in situ* polymerization.[122] Multiple active sites in the polymer chain can passivate various defects and enhance charge transfer. Meanwhile, this vast network provides adequate protection for the perovskite, stabilizing its internal structure and resisting harsh external environments, thereby delaying device degradation and minimizing the leakage of toxic lead (Fig. 7d). Other functional materials, such as ion gels and cation exchange resins, can also suppress lead leakage through their chelating ability with lead ions. These supramolecular strategies not only address the lead leakage problem but also optimize halogen stability, defect passivation, and photoelectric performance, laying the foundation for the sustainable commercialization of perovskite photovoltaics.

# 4. Summary and outlook

Supramolecular materials exhibit multidimensional potential in PSCs, leveraging non-covalent interactions to synergistically enhance performance and stability. Current research demonstrates their multifunctionality in lead immobilization (mitigating toxicity), grain-boundary passivation (enhancing charge transport), bulk structural protection (improving thermal resilience), and closed-loop lead recovery, thereby paving the way for environmentally sustainable photovoltaics.

Importantly, in addition to improvements in static efficiency, recent studies have shown that supramolecular engineering can significantly enhance device durability under real-world operating conditions (Table 1), including continuous illumination, high temperatures, electrical bias, and day–night cycles (outdoor).

Supramolecular iodine trapping, redox modulation, and host–guest confinement strategies have been shown to effectively suppress performance degradation caused by illumination and heat during maximum power point tracking and stabilize halide distribution under repeated day–night cycles, thus directly addressing failure modes associated with outdoor operation.

Table 1 The statistical table of photovoltaic parameters of PSCs based on supramolecular interactions

| Ref. | Materials | Mechanism area | PCE (%) | $V_{oc}$ (V) | $J_{sc}$ (ma cm$^{-2}$) | FF (%) | MPPT stability |
|---|---|---|---|---|---|---|---|
| 33 | β-CD | Stability enhancement | 23.2 | 1.14 | 25.4 | 79.9 | $T_{88}$ = 1000 h at 25 °C<br>$T_{80}$ = 300 h at 85 °C |
| 34 | Starch-polyiodide (Starch-I) supermolecule | Stability enhancement | 23.6 | 1.181 | 25.19 | 79.5 | T92 = 1472 h at RT<br>Retained over 98% of its initial PCE after 42 cycles of 24 h diurnal cycle operation (12 h light and 12 h dark)<br>$T_{98}$ = 1000 h in light/dark cycle test |
| 36 | HPβCD-BTCA | Lead-leakage suppression | 22.14 | 1.12 | 24.83 | 79.6 | $T_{99}$ = 700 h |
| 37 | Diazapentacene-based macrocycles | Stability enhancement | 26.13 | 1.19 | 25.82 | 85.05 | $T_{95}$ = 1000 h at 85 °C |
| 40 | Methyl-β-CD | Crystallization control | 14.94 | 1.017 | 19.67 | 74.68 | — |
| 41 | Dibenzo-30-crown-10 | Crystallization control | 21.01 | 1.30 | 18.75 | 86.18 | $T_{95}$ = 1000 h at RT |
| 93 | Crown ethers | Defect passivation | 23.70 | 1.154 | 25.8 | 79.5 | $T_{80}$ = 300 h at RT |
| 114 | 4-*tert*-butylcalix[8]arene | Defect passivation | 26.01 | 1.187 | 26.47 | 82.79 | $T_{81}$ = 1000 h at 30 °C |
| 116 | Electron-deficient biphen[*n*]arene macrocycle molecule | Defect passivation | 25.38 | 1.181 | 25.85 | 83.1 | $T_{95}$ = 1000 h at RT |
| 117 | Crown ether | Crystallization control | 20.48 | 1.061 | 24.40 | 79.19 | — |
| 118 | 4-*tert*-Butyl-1-(ethoxycarbonyl-methoxy) thiacalix[4]arene (*t*butca) | Crystallization control | 24.07 | 1.17 | 25.01 | 82.42 | — |
| 119 | β-CD-$(SH)_7$ | Stability enhancement & lead-leakage suppression | 26.14 | 1.17 | 25.72 | 86.87 | $T_{98}$ = 2780 h at 45 °C<br>$T_{85}$ = 780 h at 85 °C |
| 120 | Cationic-β-CD | Stability enhancement & lead-leakage suppression | 16.05 | 1.12 | 17.27 | 76.8 | $T_{93}$ = 1200 h at RT |
| 121 | C222 | Lead-leakage suppression | 25.34 | 1.18 | 25.81 | 83.2 | $T_{94}$ = 1500 h at RT |
| 122 | Phosphate-buffered functionalized polymer films | Lead-leakage suppression | 25.25 | 1.183 | 25.65 | 83.21 | — |

Despite significant progress, key challenges remain. Future efforts should prioritize four core directions: (1) deep mechanistic understanding, (2) rational material design, (3) multifunctional integration, and (4) application methodology innovation.

### 4.1 Deepening mechanistic understanding

Elucidating the dynamic interplay between supramolecular agents and perovskites is fundamental. Advanced *in situ* spectroscopies, super-resolution electrochemical probing, and computational modeling (DFT, MD) should be combined to resolve atomic–scale interaction mechanisms, particularly under coupled light/heat/bias stressors.

From a commercialization perspective, the ability of supramolecular systems to maintain their functionality under simultaneous illumination, thermal stress, interfacial electric fields, and repeated day–night cycling represents a decisive criterion rather than a secondary optimization target. Unlike laboratory stability tests conducted under single-stress conditions, real-world operation exposes PSCs to multiple, dynamically coupled stressors. Therefore, understanding how supramolecular interactions respond, reorganize, or self-regulate under these conditions is essential for translating efficiency records into reliable energy yield, long-term operational stability, and bankability required for industrial deployment.

### 4.2 Material innovation and rational design

Next-generation supramolecular materials must feature high $Pb^{2+}$ affinity, robust stability, and low toxicity. Examples include redox-active porphyrins and engineered cyclodextrin derivatives that can simultaneously capture iodine and remove lead. AI-assisted computational design can precisely tune energy levels and binding sites to achieve optimal perovskite compatibility. Self-healing supramolecular systems could further extend device lifetimes.

### 4.3 Multifunctional integrated architectures

The future lies in unified supramolecular platforms that concurrently enable defect passivation, crystallization control, stability enhancement, and lead containment. Hybrid systems that integrate supramolecules with conductive polymers or nanomaterials can yield synergistic effects. For instance, redox-active supramolecules embedded in hole-transport layers can simultaneously passivate defects and enhance charge extraction, thereby simplifying device architecture and reducing costs.

### 4.4 Application methodology innovation

Beyond conventional additives and post-processing methods, the effective industrialization of supramolecular strategies requires careful consideration of scalability and process compatibility. Some supramolecular materials suffer from relatively high synthesis costs, limited supply, and increased solution viscosity, which may hinder their compatibility with scalable deposition techniques such as blade coating and roll-to-roll processing. Furthermore, strong intermolecular associations and high molecular weights can adversely affect ink rheology, drying kinetics, and the uniformity of large-area films.

To address these challenges, future research should focus on low-loading supramolecular designs, interface-confined structures, and hybrid systems combining supramolecular functions with processable polymers or small molecules. Establishing compatibility with large-area coating technologies, tandem structures, and industrial encapsulation processes is crucial for bridging the gap between lab-scale devices and commercial modules.

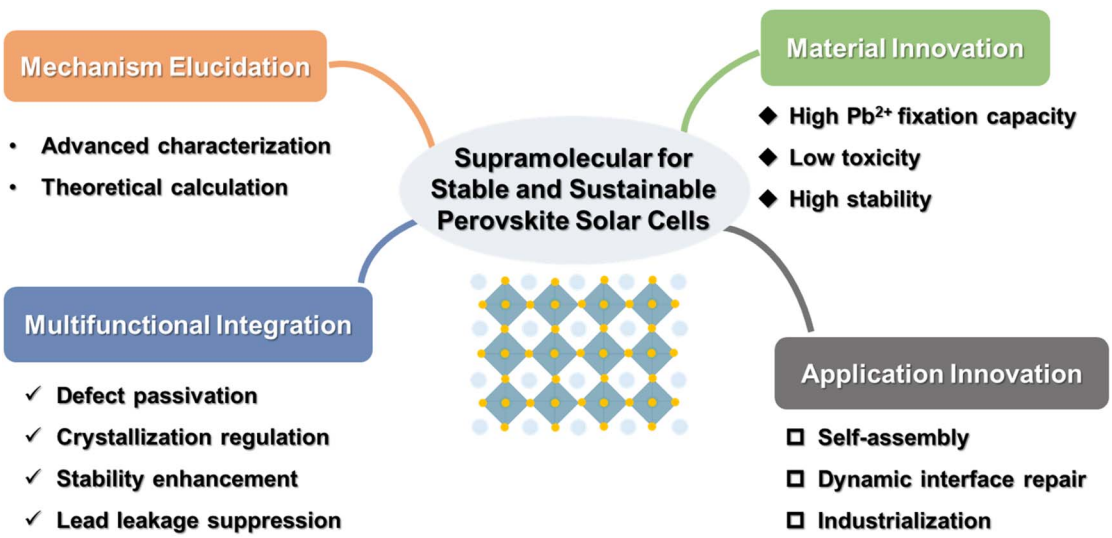


Fig. 8 Summary and outlook for the application of supramolecular materials in PSCs.

This review underscores the unique advantages of supramolecular chemistry in overcoming PSC bottlenecks. Its noncovalent, programmable nature not only introduces a new design paradigm for photovoltaics but also expands the frontiers of supramolecular science. Through coordinated advances in mechanisms, materials, and manufacturing, supramolecular engineering is poised to accelerate the commercialization of PSCs, delivering a key technological pillar for the clean energy transition and global carbon-neutrality goals (Fig. 8).

## Conflicts of interest

There are no conflicts to declare.

## Data availability

No primary research results, software or code have been included and no new data were generated or analysed as part of this review.

## Acknowledgements

A. K. Y. J. acknowledges the sponsorship of the Lee Shau-Kee Chair Professor (Materials Science) and the support from the APRC Grants (9380086, 9610419, 9610440, 9610492, 9610508) of the City University of Hong Kong; the MHKJFS Grant (MHP/054/23), TCFS grant (GHP/121/22SZ) and MRP Grant (MRP/040/21X) from the Innovation and Technology Commission of Hong Kong; and the GRF grants (11307621, 11316422, 11308625) and CRS grants (CRS_CityU104/23, CRS_HKUST203/23) from the Research Grants Council of Hong Kong. This work was partially financially supported by City University of Hong Kong (9610739) for the project "Fostering Innovation for Resilience and Sustainable Transformation," officially endorsed by the United Nations Educational, Scientific and Cultural Organization under the International Decade of Sciences for Sustainable Development (2024–2033).

## References

1 Z. Xiong, Q. Zhang, K. Cai, H. Zhou, Q. Song, Z. Han, S. Kang, Y. Li, Q. Jiang, X. Zhang and J. You, *Science*, 2025, **390**, 638–642.
2 W. Jiang, G. Qu, X. Huang, X. Chen, L. Chi, T. Wang, C.-T. Wong, F. R. Lin, C. Yang, Q. Jiang, S. Wu, J. Zhang and A. K. Y. Jen, *Nature*, 2025, **646**, 95–101.
3 L. Bi, J. Wang, Z. Zeng, X. Ji, X. Huang, F. R. Lin, S.-W. Tsang, Q. Fu and A. K. Y. Jen, *Nat. Photon.*, 2025, **19**, 968–976.
4 X. Ji, L. Bi, Q. Fu, B. Li, J. Wang, S. Y. Jeong, K. Feng, S. Ma, Q. Liao, F. R. Lin, H. Y. Woo, L. Lu, A. K. Y. Jen and X. Guo, *Adv. Mater.*, 2023, **35**, 2303665.
5 M.-I. Jamesh, H. Tong, H. Song, D. R. McKenzie, H.-Y. Hsu and P. K. Chu, *J. Power Sources*, 2026, **671**, 239554.
6 M.-I. Jamesh, H. Tong, M. Du, W. Niu, G. Jia, K.-C. Cheng, C.-W. Hsieh, H.-H. Shen, B. Xu, Y. Tian, X. Xu and H.-Y. Hsu, *npj Mater. Sustainability*, 2025, **3**, 29.
7 L. Zhang, M. Zhang, H. Wang, Z. Li, Z. Zhang, Y. Song, X. Song, S. Wang, J. Chen, W. Li, H. Dong, F. Wang, Y. Liu, X. Li, J. Yuan, W. Ma, Y. Zhang, S. Liu, F. Gao, Z. Wu, Z. Yang, F. Hao, K. Zhao, Z. Jin, K. Yan, J. Chang, J. Cao, J. Wang, X. Zhang, Q. Dong, P. Gao, Y. Zhao, L. Xiao, Y. Ding and L. Ding, *Adv. Mater.*, 2025, e12221.
8 S. Wang, H. Lian, Y. Yang, Z. Wu, Y. Li, H. Ling, W. Pisula, T. Marszalek and T. Xu, *FlexMat*, 2025, **2**, 82–106.
9 X. Cheng, Z. Dou, H. Lian, Z. Qin, H. Guo, X. Li, W.-Y. Wong and Q. Dong, *FlexMat*, 2024, **1**, 127–149.
10 M. A. Green, A. Ho-Baillie and H. J. Snaith, *Nat. Photon.*, 2014, **8**, 506–514.
11 S. D. Stranks, G. E. Eperon, G. Grancini, C. Menelaou, M. J. P. Alcocer, T. Leijtens, L. M. Herz, A. Petrozza and H. J. Snaith, *Science*, 2013, **342**, 341–344.
12 Z. Saki, M. M. Byranvand, N. Taghavinia, M. Kedia and M. Saliba, *Energy Environ. Sci.*, 2021, **14**, 5690–5722.
13 C. Yang, W. Hu, J. Liu, C. Han, Q. Gao, A. Mei, Y. Zhou, F. Guo and H. Han, *Light Sci. Appl.*, 2024, **13**, 227.
14 X. Sun, W. Shi, T. Liu, J. Cheng, X. Wang, P. Xu, W. Zhang, X. Zhao and W. Guo, *Science*, 2025, **388**, 957–963.
15 J. Wang, L. Bi, Q. Fu and A. K. Y. Jen, *Adv. Energy Mater.*, 2024, **14**, 2401414.
16 K. Sakhatskyi, R. A. John, A. Guerrero, S. Tsarev, S. Sabisch, T. Das, G. J. Matt, S. Yakunin, I. Cherniukh, M. Kotyrba, Y. Berezovska, M. I. Bodnarchuk, S. Chakraborty, J. Bisquert and M. V. Kovalenko, *ACS Energy Lett.*, 2022, **7**, 3401–3414.
17 H. Wang, Y. Liu, Y. Xiao, J. Jia, C. Liu, H. Chen, W. Yan and M. Zhu, *Adv. Funct. Mater.*, 2025, e23571.
18 J. Huang, S. Tan, P. D. Lund and H. Zhou, *Energy Environ. Sci.*, 2017, **10**, 2284–2311.
19 C. Tian, T. Wu, X. Zhou, Y. Xu, B. Li, Z. Zhang, K. Li, C. Hou, Y. Li, H. Wang and Q. Zhang, *Adv. Funct. Mater.*, 2025, e24518.
20 X. Ji, Y. Ding, L. Bi, X. Yang, J. Wang, X. Wang, Y. Liu, Y. Yan, X. Zhu, J. Huang, L. Yang, Q. Fu, A. K. Y. Jen and L. Lu, *Angew. Chem., Int. Ed.*, 2024, **63**, e202407766.
21 T. J. Silverman, M. G. Deceglie, I. Repins, M. Owen-Bellini, J. J. Berry, J. S. Stein and L. T. Schelhas, *Nat. Energy*, 2025, **10**, 934–940.
22 B. Yan, W. Dai, Z. Wang, Z. Zhong, L. Zhang, M. Yu, Q. Zhou, Q. Ma, K. Yan, L. Zhang, Y. Yang and J. Yao, *Science*, 2025, **388**, eadt5001.
23 T.-S. Su, A. Krishna, C. Zhao, J. Chu and H. Zhang, *Chem. Soc. Rev.*, 2025, **54**, 6448–6481.
24 P. Ximenis, D. Martínez, L. Rubert and B. Soberats, *Chem. Soc. Rev.*, 2025, **54**, 11659–11698.
25 F. Li, X. Deng, Z. Shi, S. Wu, Z. Zeng, D. Wang, Y. Li, F. Qi, Z. Zhang, Z. Yang, S.-H. Jang, F. R. Lin, S. W. Tsang, X.-K. Chen and A. K. Y. Jen, *Nat. Photon.*, 2023, **17**, 478–484.
26 J. Wang, W. Lin, V. O. Nikolaeva, R. Javaid and N. M. Khashab, *Nat. Commun.*, 2025, **16**, 7618.
27 C.-Y. Shi, Q. Zhang, H. Tian and D.-H. Qu, *SmartMat*, 2020, **1**, e1012.
28 Z. Fang, L. Wang, X. Mu, B. Chen, Q. Xiong, W. D. Wang, J. Ding, P. Gao, Y. Wu and J. Cao, *J. Am. Chem. Soc.*, 2021, **143**, 18989–18996.

29 X. Chen, C. Deng, J. Wu, Q. Chen, Y. Du, Y. Xu, R. Li, L. Tan, Y. Wei, Y. Huang and Z. Lan, *Adv. Funct. Mater.*, 2024, **34**, 2311527.
30 J. Li, X. Qiao, B. He, Y. Zhang, S. Pal, L. Sun, M. Bilal, Z. Su, X. Gao, J. Briscoe, I. Abrahams, M. Li, Z. Li and Y. Lu, *Energy Environ. Sci.*, 2025, **18**, 5632–5642.
31 Z. Zhang, Y. Yang, Z. Huang, Q. Xu, S. Zhu, M. Li, P. Zhao, H. Cui, S. Li, X. Jin, X. Wu, M. Han, Y. Zhang, N. Zhao, C. Zou, Q. Liang, L. Xian, J. Hu, C. Zhu, Y. Chen, Y. Bai, Y. Li, Q. Chen, H. Zhou, B. Zhang and Y. Jiang, *Energy Environ. Sci.*, 2024, **17**, 7182–7192.
32 G. Xu, I. Muhammad, Y. Zhang, X. Zheng, M. Xin, H. Gao, J. Li, C. Liu, W. Chen, J. Tang, F. Yang, Y. Su, P. Han, Y. Sheng, D. Khan, X. Wang and Z. Tang, *Adv. Energy Mater.*, 2025, **15**, 2405088.
33 X. Li, H. Yang, A. Liu, C. Lu, H. Yuan, W. Zhang and J. Fang, *Energy Environ. Sci.*, 2023, **16**, 6071–6077.
34 Y. Zhang, Q. Song, G. Liu, Y. Chen, Z. Guo, N. Li, X. Niu, Z. Qiu, W. Zhou, Z. Huang, C. Zhu, H. Zai, S. Ma, Y. Bai, Q. Chen, W. Huang, Q. Zhao and H. Zhou, *Nat. Photon.*, 2023, **17**, 1066–1073.
35 C. Tian, T. Wu, X. Zhou, Y. Zhao, B. Li, X. Han, K. Li, C. Hou, Y. Li, H. Wang and Q. Zhang, *Adv. Mater.*, 2025, **37**, 2411982.
36 M. Yang, T. Tian, Y. Fang, W.-G. Li, G. Liu, W. Feng, M. Xu and W.-Q. Wu, *Nat. Sustain.*, 2023, **6**, 1455–1464.
37 Y. Wu, W. Li, S. Li, Y.-F. Niu, C. Wang, H.-B. Yang, X.-L. Zhao, X. Li, J. Fang and X. Shi, *Adv. Sci.*, 2025, e16964.
38 Z. Fang, X. Mu, G.-B. Xiao and J. Cao, *Angew. Chem., Int. Ed.*, 2025, **64**, e202418834.
39 H. Guo, X. Wang, C. Li, H. Hu, H. Zhang, L. Zhang, W.-H. Zhu and Y. Wu, *Adv. Mater.*, 2023, **35**, 2301871.
40 M. Zeng, Z. Yan, X. Ye, Y. Lou, T. Sheng, X. Jiang, Y. Mao, A. Huang, X. Yang, Z. Wang, Y. Sun, Y. Bai, H.-M. Cheng and G. Xing, *ACS Energy Lett.*, 2025, **10**, 1357–1365.
41 X. Lian, M. Jin, W. Dai, Y. Lv, M. Luo, Y. Hu, Z. Wang, H. Li, C. Xu, D. Jiang, H. Min, Y. Chen, J. Chang, T.-S. Su, F. Ma, Y. Bai, H. Zhang, X. Mo and J. Chu, *Nat. Commun.*, 2025, **16**, 7173.
42 K. J. Prince, H. M. Mirletz, E. A. Gaulding, L. M. Wheeler, R. A. Kerner, X. Zheng, L. T. Schelhas, P. Tracy, C. A. Wolden, J. J. Berry, S. Ovaitt, T. M. Barnes and J. M. Luther, *Nat. Mater.*, 2025, **24**, 22–33.
43 J.-M. Lehn, *Angew. Chem., Int. Ed.*, 1988, **27**, 89–112.
44 C. A. Hunter, *Angew. Chem., Int. Ed.*, 2004, **43**, 5310–5324.
45 G. M. Whitesides and B. Grzybowski, *Science*, 2002, **295**, 2418–2421.
46 J.-M. Lehn, *Angew. Chem., Int. Ed.*, 1990, **29**, 1304–1319.
47 B. C. Gibb, *Nat. Chem.*, 2020, **12**, 665–667.
48 A. L. Thompson and N. G. White, *Chem. Soc. Rev.*, 2023, **52**, 6254–6269.
49 L. Chen, J. Xu, M. Zhu, Z. Zeng, Y. Song, Y. Zhang, X. Zhang, Y. Deng, R. Xiong and C. Huang, *Mater. Horiz.*, 2023, **10**, 4000–4032.
50 F. Li, X. Huang, C. Ma, J. Xue, Y. Li, D. Kim, H.-S. Yang, Y. Zhang, B. R. Lee, J. Kim, B. Wu and S. H. Park, *Adv. Sci.*, 2023, **10**, 2301603.
51 D. Wang, Z. Liu, Z.-W. Gao, X. Lei, P. Zhu, J. Zeng, Q. Li, L. Wang, Z. Zhang, M. Gu, S. He, Y. Bao, Q. Lian, J. Li, Z. Song, Y. Xu, D. Lei, X. Wang, A. K. Y. Jen and B. Xu, *Nat. Energy*, 2026, DOI: 10.1038/s41560-026-01964-4.
52 T. Yong, S. Choi, S.-K. Kim, S. Han, G. Seo, H. J. Kim, J. Y. Park, H. N. Yu, H. R. You, E. J. Lee, G. Lee, W. Lee, S. Kim, S. Yun, Y. Lee, J. Lee, D.-H. Kim, S. J. Lim, D.-H. Nam, Y. Kim, J. Lim, B. J. Moon and J. Choi, *Energy Environ. Sci.*, 2024, **17**, 9443–9454.
53 M. Li, R. Sun, J. Chang, J. Dong, Q. Tian, H. Wang, Z. Li, P. Yang, H. Shi, C. Yang, Z. Wu, R. Li, Y. Yang, A. Wang, S. Zhang, F. Wang, W. Huang and T. Qin, *Nat. Commun.*, 2023, **14**, 573.
54 C. Liu, Y. Yang, H. Chen, I. Spanopoulos, A. S. R. Bati, I. W. Gilley, J. Chen, A. Maxwell, B. Vishal, R. P. Reynolds, T. E. Wiggins, Z. Wang, C. Huang, J. Fletcher, Y. Liu, L. X. Chen, S. De Wolf, B. Chen, D. Zheng, T. J. Marks, A. Facchetti, E. H. Sargent and M. G. Kanatzidis, *Nature*, 2024, **633**, 359–364.
55 S. Kawai, A. S. Foster, T. Björkman, S. Nowakowska, J. Björk, F. F. Canova, L. H. Gade, T. A. Jung and E. Meyer, *Nat. Commun.*, 2016, **7**, 11559.
56 Z. Yang, Y. Jiang, Y. Wang, G. Li, Q. You, Z. Wang, X. Gao, X. Lu, X. Shi, G. Zhou, J.-M. Liu and J. Gao, *Small*, 2024, **20**, 2307186.
57 I. C. Ribeiro, P. I. R. Moraes, A. F. B. Bittencourt and J. L. F. Da Silva, *J. Phys. Chem. C*, 2023, **127**, 13667–13677.
58 L. Bi, Q. Fu, Z. Zeng, Y. Wang, F. R. Lin, Y. Cheng, H.-L. Yip, S. W. Tsang and A. K. Y. Jen, *J. Am. Chem. Soc.*, 2023, **145**, 5920–5929.
59 Z. Wen, C. Liang, S. Li, G. Wang, B. He, H. Gu, J. Xie, H. Pan, Z. Su, X. Gao, G. Hong and S. Chen, *Energy Environ. Mater.*, 2024, **7**, e12680.
60 Y. Liu, X. Yang, X. Ding, J. Wang, W. Xu, X. Wang, L. Zhang, Y. Yan, J. Wang, Y. Hou, L. Yang, T. Chu, Q. Jiang, X. Zhu, Z. Hu, B. Kan, X. Gao, Q. Fu, L. Yang, Z. Chen, S. Shao, L. Lu and X. Ji, *Small*, 2025, **21**, 2502367.
61 D. Koo, Y. Choi, U. Kim, J. Kim, J. Seo, E. Son, H. Min, J. Kang and H. Park, *Nat. Nanotechnol.*, 2025, **20**, 75–82.
62 F. Hu, C.-H. Chen, T.-Y. Teng, Y.-R. Shi, B. Wang, D. Xue, Y. Xia, J. Chen, K.-L. Wang, L.-Z. Huang, I. Yavuz, Z.-K. Wang and L.-S. Liao, *Adv. Energy Mater.*, 2024, **14**, 2302926.
63 K. Li, Z. Huang, H. Zai, Z. Zhang, F. Wang, X. Zhu, Y. Wu, Y. Zhang, F. Pei, R. Fan, X. Niu, Y. Chen, H. Liu, R. Yin, X. Zhuang, J. A. Steele, C. Zhu, Y. Chen, T. Song, Q. Chen and H. Zhou, *Adv. Mater.*, 2025, **38**, e17685.
64 H. Zhang, F. T. Eickemeyer, Z. Zhou, M. Mladenović, F. Jahanbakhshi, L. Merten, A. Hinderhofer, M. A. Hope, O. Ouellette, A. Mishra, P. Ahlawat, D. Ren, T.-S. Su, A. Krishna, Z. Wang, Z. Dong, J. Guo, S. M. Zakeeruddin, F. Schreiber, A. Hagfeldt, L. Emsley, U. Rothlisberger, J. V. Milić and M. Grätzel, *Nat. Commun.*, 2021, **12**, 3383.
65 H. Zai, P. Yang, J. Su, R. Yin, R. Fan, Y. Wu, X. Zhu, Y. Ma, T. Zhou, W. Zhou, Y. Zhang, Z. Huang, Y. Jiang, N. Li, Y. Bai, C. Zhu, Z. Huang, J. Chang, Q. Chen, Y. Zhang and H. Zhou, *Science*, 2025, **387**, 186–192.

66 K. Carter-Fenk, M. Liu, L. Pujal, M. Loipersberger, M. Tsanai, R. M. Vernon, J. D. Forman-Kay, M. Head-Gordon, F. Heidar-Zadeh and T. Head-Gordon, *J. Am. Chem. Soc.*, 2023, **145**, 24836–24851.
67 Q. Fu, H. Liu, S. Li, T. Zhou, M. Chen, Y. Yang, J. Wang, R. Wang, Y. Chen and Y. Liu, *Angew. Chem., Int. Ed.*, 2022, **61**, e202210356.
68 K. Feng, G. Wang, Q. Lian, S. Gámez-Valenzuela, B. Li, R. Ding, W. Yang, K. Wang, J. Zeng, Y. Zhang, S. Y. Jeong, B. Xu, A. Ho-Baillie, H. Y. Woo, A. Facchetti and X. Guo, *Nat. Mater.*, 2025, **24**, 770–777.
69 T. Zhao, X. Jin, M.-H. Li, J. Li, S. Wang, Z. Zhang, P. Sun, S. Lin, Q. Chen, J.-S. Hu, Y. Li and Y. Jiang, *J. Am. Chem. Soc.*, 2024, **146**, 30893–30900.
70 L. Wang, S. Yuan, F. Qian, T. Zhang, H. Zheng, X. Li, T. Lan, Q. Xu, P. Zhang and S. Li, *Energy Environ. Sci.*, 2024, **17**, 8337–8348.
71 Q. Fu, X. Tang, H. Liu, R. Wang, T. Liu, Z. Wu, H. Y. Woo, T. Zhou, X. Wan, Y. Chen and Y. Liu, *J. Am. Chem. Soc.*, 2022, **144**, 9500–9509.
72 X. Ji, T. Zhou, Q. Fu, W. Wang, Z. Wu, M. Zhang, X. Guo, D. Liu, H. Y. Woo and Y. Liu, *Adv. Energy Mater.*, 2023, **13**, 2203756.
73 H. Jiang, G. Yang, X. Wang, Y. Wang, A. Zhang, H. Lu, C. Zhang, L. Cao, D. Ouyang and Z. Bo, *J. Am. Chem. Soc.*, 2025, **147**, 46039–46050.
74 X. Wang, S. Yuan, S. Lu, Z. Liang, S. Zhang, R. Lv, X. Li, H. Fan, W. Chen, X. Han, Y. Li, C. Zhang, X. Pan, T. Chen, Z. Xiao, Q. He, F. Li, Z. Fang, X. C. Zeng, Z. Zhu and S. Yang, *Natl. Sci. Rev.*, 2025, **12**, nwaf466.
75 Q. Li, Y. Zheng, H. Wang, X. Liu, M. Lin, X. Sui, X. Leng, D. Liu, Z. Wei, M. Song, D. Li, H. G. Yang, S. Yang and Y. Hou, *Science*, 2025, **387**, 1069–1077.
76 Y. Lin, Z. Lin, S. Lv, Y. Shui, W. Zhu, Z. Zhang, W. Yang, J. Zhao, H. Gu, J. Xia, D. Wang, F. Du, A. Zhu, J. Liu, H. Cai, B. Wang, N. Zhang, H. Wang, X. Liu, T. Liu, C. Kong, D. Zhou, S. Chen, Z. Yang, T. Li, W. Ma, G. Fang, L. Echegoyen, G. Xing, S. Yang, T. Yang, W. Cai, M. Li, W. Huang and C. Liang, *Nature*, 2025, **642**, 78–84.
77 J. Sun, J. Wang, Z.-F. Yao, L. Bi, X. Ji, J. Wang, X. Huang, M. Liu, K. Liu, F. R. Lin, B. Kan, Q. Fu and A. K. Y. Jen, *J. Am. Chem. Soc.*, 2025, **147**, 31965–31974.
78 Z. Huang, Y. Bai, X. Huang, J. Li, Y. Wu, Y. Chen, K. Li, X. Niu, N. Li, G. Liu, Y. Zhang, H. Zai, Q. Chen, T. Lei, L. Wang and H. Zhou, *Nature*, 2023, **623**, 531–537.
79 Q. Fu, M. Chen, Q. Li, H. Liu, R. Wang and Y. Liu, *J. Am. Chem. Soc.*, 2023, **145**, 21687–21695.
80 J. Wang, L. Bi, X. Huang, Q. Feng, M. Liu, M. Chen, Y. An, W. Jiang, F. R. Lin, Q. Fu and A. K. Y. Jen, *eScience*, 2024, **4**, 100308.
81 Y. Gao, H. Liu, Z. Song, Y. Chen, L. Yang, Z. Hu, Y. Zou, Y. Chen and Y. Liu, *Nat. Photon.*, 2026, **20**, 178–185.
82 Q. Fu, X. Ji, S. Tian, B. Jiang, L. Tao, L. Bi, L. Lu, P. J. Dyson, Y. Ding, M. K. Nazeeruddin and A. K. Y. Jen, *Mater. Today*, 2025, **89**, 192–205.
83 Q. Fu, Z. Xu, X. Tang, T. Liu, X. Dong, X. Zhang, N. Zheng, Z. Xie and Y. Liu, *ACS Energy Lett.*, 2021, **6**, 1521–1532.
84 H. Lai, X. Yang, L. Zhang, L. Bi, B. Tian, H. Wang, X. Gao, L. Lu, B. Kan, X. Ji and Q. Fu, *Chem. Eng. J.*, 2024, **489**, 151383.
85 W. Jiang, F. Li, M. Li, F. Qi, F. R. Lin and A. K. Y. Jen, *Angew. Chem., Int. Ed.*, 2022, **61**, e202213560.
86 X. Huang, L. Bi, Z. Yao, Q. Fu, B. Fan, S. Wu, Z. Su, Q. Feng, J. Wang, Y. Hong, M. Liu, Y. An, M. Chen and A. K. Y. Jen, *Adv. Mater.*, 2024, **36**, 2410564.
87 R. Li, J. Ding, X. Mu, Y. Kang, A. Wang, W. Bi, Y. Zhang, J. Cao and Q. Dong, *J. Energy Chem.*, 2022, **71**, 141–149.
88 Q. Jiang, Y. Zhao, X. Zhang, X. Yang, Y. Chen, Z. Chu, Q. Ye, X. Li, Z. Yin and J. You, *Nat. Protoc.*, 2019, **13**, 460–466.
89 F. Wang, X. Li, H. Wang, Y. Gou, S. Yang, D. Han, L. Yang, L. Fan, J. Yang and F. Rosei, *Chem. Eng. J.*, 2022, **446**, 137431.
90 Y. Wang, Y. Meng, C. Liu, R. Cao, B. Han, L. Xie, R. Tian, X. Lu, Z. Song, J. Li, S. Yang, C. Lu and Z. Ge, *Joule*, 2024, **8**, 1120–1141.
91 D. J. Cram, *Science*, 1988, **240**, 760–767.
92 H. Zhu, L. Chen, B. Sun, M. Wang, H. Li, J. F. Stoddart and F. Huang, *Nat. Rev. Chem.*, 2023, **7**, 768–782.
93 T.-S. Su, F. T. Eickemeyer, M. A. Hope, F. Jahanbakhshi, M. Mladenović, J. Li, Z. Zhou, A. Mishra, J.-H. Yum, D. Ren, A. Krishna, O. Ouellette, T.-C. Wei, H. Zhou, H.-H. Huang, M. D. Mensi, K. Sivula, S. M. Zakeeruddin, J. V. Milić, A. Hagfeldt, U. Rothlisberger, L. Emsley, H. Zhang and M. Grätzel, *J. Am. Chem. Soc.*, 2020, **142**, 19980–19991.
94 S.-J. Kim, Y. Kim, R. K. Chitumalla, G. Ham, T.-D. Nguyen, J. Jang, H. Cha, J. Milić, J.-H. Yum, K. Sivula and J.-Y. Seo, *J. Energy Chem.*, 2024, **92**, 263–270.
95 K. Freudenberg, M. Meyer-Delius and B. Dtsch, *Chem. Ges.*, 1938, **71**, 1596–1600.
96 J. Szejtli, *Chem. Rev.*, 1998, **98**, 1743–1754.
97 A. M. Musuc, *Molecules*, 2024, **29**, 5319.
98 J. Wang, D. Li, X. Li, G. Liu, Y. Zhu, L. Sun and F. Li, *Chem*, 2025, **11**, 102365.
99 P. Ferdowsi, S.-J. Kim, T.-D. Nguyen, J.-Y. Seo, J.-H. Yum and K. Sivula, *J. Mater. Chem. A*, 2024, **12**, 15837–15846.
100 S. Masi, F. Aiello, A. Listorti, F. Balzano, D. Altamura, C. Giannini, R. Caliandro, G. Uccello-Barretta, A. Rizzo and S. Colella, *Chem. Sci.*, 2018, **9**, 3200–3208.
101 A. A. H. Abdellatif, F. Ahmed, A. M. Mohammed, M. Alsharidah, A. Al-Subaiyel, W. A. Samman, A. A. Alhaddad, S. H. Al-Mijalli, M. A. Amin, H. Barakat and S. K. Osman, *Int. J. Nanomed.*, 2023, **18**, 3247–3281.
102 C. Xing, X. Zheng, T. Deng, L. Zeng, X. Liu and X. Chi, *Pharmaceutics*, 2023, **15**, 5.
103 G. W. Gokel, W. M. Leevy and M. E. Weber, *Chem. Rev.*, 2004, **104**, 2723–2750.
104 J. Gui, Y. Wang, Q. Li, Q. Chen, L. Wang, Y. Xu, G. Yao, L. Fan, K.-Z. Du, R. Sa, Z. Su and Y. Xiao, *Adv. Opt. Mater.*, 2025, **13**, 2402175.
105 Z. Liu, S. K. M. Nalluri and J. F. Stoddart, *Chem. Soc. Rev.*, 2017, **46**, 2459–2478.
106 F. Ullah, T. A. Khan, J. Iltaf, S. Anwar, M. F. Khan, M. R. Khan, S. Ullah, M. Fayyaz ur Rehman,

M. Mustaqeem, K. Kotwica-Mojzych and M. Mojzych, *Appl. Sci.*, 2022, **12**, 1102.

107 J. S. Bradshaw and R. M. Izatt, *Acc. Chem. Res.*, 1997, **30**, 338–345.

108 X. Huang, D. Xia, Q. Xie, D. Wang, Q. Li, C. Zhao, J. Yin, F. Cao, Z. Su, Z. Zeng, W. Jiang, W. Kaminsky, K. Liu, F. R. Lin, Q. Feng, B. Wu, S.-W. Tsang, D. Lei, W. Li and A. K. Y. Jen, *Nat. Commun.*, 2025, **16**, 1626.

109 (*a*) X. Liu, J. Xie, Z. Zhou, H. Lian, X. Sui, Q. Li, M. Lin, D. Liu, H. Yuan, F. Gao, Y. Wu, H. G. Yang, S. Yang and Y. Hou, *Nano-Micro Lett.*, 2025, **18**, 67; (*b*) C. Marquez, H. Fang and W. M. Nau, *IEEE Trans. NanoBioscience*, 2004, **3**, 39–45.

110 J. Lagona, P. Mukhopadhyay, S. Chakrabarti and L. Isaacs, *Angew. Chem., Int. Ed.*, 2005, **44**, 4844–4870.

111 N. Liu, J. Duan, H. Li, L. Ma, B. Wang, J. Li, X. Duan, Q. Guo, J. Dou, S. Geng, Y. Liu, C. Zhang, Y. Liu, B. He, X. Yang and Q. Tang, *Adv. Energy Mater.*, 2024, **14**, 2402443.

112 M. A. Ruiz-Preciado, D. J. Kubicki, A. Hofstetter, L. McGovern, M. H. Futscher, A. Ummadisingu, R. Gershoni-Poranne, S. M. Zakeeruddin, B. Ehrler, L. Emsley, J. V. Milić and M. Grätzel, *J. Am. Chem. Soc.*, 2020, **142**, 1645–1654.

113 M. A. Hope, T. Nakamura, P. Ahlawat, A. Mishra, M. Cordova, F. Jahanbakhshi, M. Mladenović, R. Runjhun, L. Merten, A. Hinderhofer, B. I. Carlsen, D. J. Kubicki, R. Gershoni-Poranne, T. Schneeberger, L. C. Carbone, Y. Liu, S. M. Zakeeruddin, J. Lewinski, A. Hagfeldt, F. Schreiber, U. Rothlisberger, M. Grätzel, J. V. Milić and L. Emsley, *J. Am. Chem. Soc.*, 2021, **143**, 1529–1538.

114 D. He, D. Ma, J. Zhang, Y. Yang, J. Ding, C. Liu, X. Liu, Y. Yu, T. Liu, C. Chen, M. Li and J. Chen, *Adv. Mater.*, 2025, **37**, 2505115.

115 G. Yang, X. Liu, L. Wang, K. Dong, B. Zhang, X. Jiang, Y. Yin, M. Wang, W. Niu, L. Zheng, S. Yu, S. Liu, S. M. Zakeeruddin, X. Guo, S. Pang, L. Sun, M. Grätzel and M. Wei, *Angew. Chem., Int. Ed.*, 2024, **63**, e202410454.

116 J. Qiu, H. Zhu, B. Shao, Y. Shi, S. Xu, M. Abulikemu, J. Liu, Z. Zheng, A. Jamal, H. A. Alsaiari, S. Aqeel, I. Gereige, F. Zhang, J. Yin, C. Li and O. M. Bakr, *J. Am. Chem. Soc.*, 2025, **147**, 42061–42069.

117 R. Chen, Y. Wu, Y. Wang, R. Xu, R. He, Y. Fan, X. Huang, J. Yin, B. Wu, J. Li and N. Zheng, *Adv. Funct. Mater.*, 2021, **31**, 2008760.

118 N. Zhang, T. Li, C. Wang, Q. Xiong, F. Li, Z. Zhang, C. Deng, C. Hu, N. Shibayama, J. Wu and P. Gao, *Adv. Funct. Mater.*, 2023, **33**, 2300830.

119 J. Wang, X.-Y. Dai, L. Bi, J. Sun, M. Liu, X. Ji, F. R. Lin, Q. Fu and A. K. Y. Jen, *Joule*, 2025, **9**, 102105.

120 M. Yang, Y. Tan, G. Yang, X. Chang, T. Tian, W.-G. Li, Y. Fang, J. Shen, S. Yang and W.-Q. Wu, *Angew. Chem., Int. Ed.*, 2025, **64**, e202415966.

121 Q. Zhuang, Z. Xu, H. Li, C. Zhang, C. Gong, H. Wang, X. Li and Z. Zang, *Sci. Adv.*, 2025, **11**, eado7318.

122 J. Ma, S. Fan, C. Shao, L. Wang, Y. Dong, G. Niu, Z. Nie, S. Yang, J. Wang and H. Yang, *Angew. Chem., Int. Ed.*, 2025, **64**, e202425578.

123 Q. Zhuang, K. Wang, H. Li, Z. Liu, Y. Li, Y. Yang, Q. Lin, C. Gong, C. Zhang, Z. Guo, S. M. H. Qaid, I. Mora-Seró, Z. Xu, Z. Zang and H. Wang, *Nano Energy*, 2025, **134**, 110547.

124 X. Jin, J. Li, S. Zhu, W. Tan, J. Tang, X. Gong, X. Liu, Y. Zhang, C. Zhou, Z. Tang, V. O. Nyamori, B. S. Martincigh, M. L. Davies, M. Li, T. Chen, Q. Chen, J. Hu, Q. Liang, W. Chen and Y. Jiang, *Energy Environ. Sci.*, 2025, **18**, 1901–1910.

125 H. Luo, J. Ma, P. Gao, S. Wang, R. Zhao, J. Yang, Y. Li, P. Zhou, Q. Xu, R. Zhu, Z. Liu, X. Li, W. Chen, Y. Song and Y. Zhang, *Adv. Mater.*, 2025, **37**, 2506206.

126 S. Wang, T. Xin, Y. Zhao, W. Liu, L. Bu, X. Li and G. Lu, *Sci. Adv.*, 2025, **11**, eadw1437.

127 (*a*) S. S. Dipta, A. J. Christofferson, P. V. Kumar, V. Kundi, M. Hanif, J. Tang, N. Flores, K. Kalantar-Zadeh, A. Uddin and M. A. Rahim, *Adv. Sci.*, 2024, **11**, 2403057; (*b*) H. Cheng, Y. Li, P. Mao, J. Lv, M. Li, S. Xing, P.-C. Yang and Y. Zhong, *ACS Sustain. Chem. Eng.*, 2025, **13**, 16204–16210.

128 S. Wu, Z. Li, M.-Q. Li, Y. Diao, F. Lin, T. Liu, J. Zhang, P. Tieu, W. Gao, F. Qi, X. Pan, Z. Xu, Z. Zhu and A. K. Y. Jen, *Nat. Nanotechnol.*, 2020, **15**, 934–940.

129 Y. Zhang, T. Wang, H. Chen, J. Yang, Y. Wang, R. Yin, W. Chen, J. Su, X. Hu, W. Zhong, L. Shang, F. Yan, M.-M. Titirici, B. Wei and X. Li, *Sci. China Chem.*, 2026, **69**, 1016–1022.

130 H. Liu, Z. Zhang, Y. Shi, W. Ran, H. Zhong and F. Zhang, *Joule*, 2025, **9**, 101816.

131 K. Liu, T. Hu, Z. Cai, F. Liu, S. Rafique, X. Li, L. Deng, C. Li, Y. Wang, Q. Guo, X. Yue, J. Wang, Y. Yang, C. Cong, S. Chen, J. Zhang, A. Yu and Y. Zhan, *Energy Environ. Sci.*, 2024, **17**, 5576–5587.

132 S. Chen, Y. Deng, H. Gu, S. Xu, S. Wang, Z. Yu, V. Blum and J. Huang, *Nat. Energy*, 2020, **5**, 1003–1011.